Parasitology Research (2020) 119:2943–2954
https://doi.org/10.1007/s00436-020-06779-0

PROTOZOOLOGY - ORIGINAL PAPER

Repositioning of leishmanicidal [1,2,3]Triazolo[1,5-*a*]pyridinium salts for Chagas disease treatment: *Trypanosoma cruzi* cell death involving mitochondrial membrane depolarisation and Fe-SOD inhibition

Rubén Martín-Escolano[1] · Javier Martín-Escolano[1] · Rafael Ballesteros-Garrido[2] · Nuria Cirauqui[3] · Belén Abarca[2] · María José Rosales[1] · Manuel Sánchez-Moreno[1] · Rafael Ballesteros[2] · Clotilde Marín[1]

Received: 18 December 2019 / Accepted: 18 June 2020 / Published online: 1 July 2020

Abstract

Trypanosomatidae is a family of unicellular parasites belonging to the phylum Euglenozoa, which are causative agents in high impact human diseases such as Leishmaniasis, Chagas disease and African sleeping sickness. The impact on human health and local economies, together with a lack of satisfactory chemotherapeutic treatments and effective vaccines, justifies stringent research efforts to search for new disease therapies. Here, we present in vitro trypanocidal activity data and mode of action data, repositioning leishmanicidal [1,2,3]Triazolo[1,5-*a*]pyridinium salts against *Trypanosoma cruzi*, the aetiological agent of Chagas disease. This disease is one of the most neglected tropical diseases and is a major public health issue in Central and South America. The disease affects approximately 6–7 million people and is widespread due to increased migratory movements. We screened a suite of leishmanicidal [1,2,3]Triazolo[1,5-*a*]pyridinium salt compounds, of which compounds **13**, **20** and **21** were identified as trypanocidal drugs. These compounds caused cell death in a mitochondrion-dependent manner through a bioenergetic collapse. Moreover, compounds **13** and **20** showed a remarkable inhibition of iron superoxide dismutase activity of *T. cruzi*, a key enzyme in the protection from the damage produced by oxidative stress.

Keywords Chagas disease · Chemotherapy · Pyridines · Superoxide dismutase · Trypanocidal agents · *Trypanosoma cruzi*

Section Editor: Sarah Hendrickx

Electronic supplementary material The online version of this article (https://doi.org/10.1007/s00436-020-06779-0) contains supplementary material, which is available to authorized users.

✉ Clotilde Marín
cmaris@ugr.es

Belén Abarca
belen.abarca@uv.es

Rafael Ballesteros
rafael.ballesteros@uv.es

[1] Department of Parasitology, Instituto de Investigación Biosanitaria (ibs. Granada), Hospitales Universitarios de Granada/University of Granada, Severo Ochoa s/n, 18071 Granada, Spain

[2] Departamento de Química Orgánica, Facultad de Farmacia, Universidad de Valencia, Avda. Vicente Andrés Estellés s/n, 46100 Burjassot, Valencia, Spain

[3] Molecular Microbiology and Structural Biochemistry, Centre National de la Recherche Scientifique, Université Claude Bernard Lyon 1, 69367 Lyon Cedex 07, France

Introduction

Trypanosomatidae is a family of unicellular and uniflagellated parasites that cause human diseases such as leishmaniasis, American trypanosomiasis or Chagas disease (CD) and African sleeping sickness. All are classified as neglected tropical diseases (NTDs) caused by infection with insect-transmitted protozoan parasites (WHO 2019). CD is a life-long and life-threatening disease and is an important public health issue in Central and South America. CD is a major cause of morbidity and mortality in several endemic regions (Moncayo and Silveira 2009; Hashimoto and Yoshioka 2012; Bern 2015). In recent years, CD has become a recognised and widespread parasitic disease due to increased migratory movements, particularly in the USA and Europe (Bern and Montgomery 2009; Bern et al. 2011; L. et al. 2011; Pérez-Molina et al. 2012; Requena-Méndez et al. 2015).

The aetiological agent of CD is the protozoan parasite *Trypanosoma cruzi*, a parasite with a complex life cycle

where four different morphological forms alternate between the triatomine vector and the mammalian host. The main route of transmission is through these vectors, although other routes such as oral, congenital, transplants and transfusions are also important (Bastos et al. 2010; Blanchet et al. 2014; Hernández et al. 2016). *Trypanosoma cruzi* is an obligate intracellular parasite in mammalian hosts, and its infection is far from innocuous (Kessler et al. 2017; Tyler and Engman 2001). During the acute phase, *T. cruzi* is detected in the bloodstream and spreads to tissues and organs, usually manifesting as a mild febrile illness. Subsequently, the parasite burden becomes extremely low, and CD progresses to a long-lasting asymptomatic phase (Cardillo et al. 2015; Tarleton 2015). Finally, in approximately 30% of cases, the disease moves to a symptomatic phase, where cardiomyopathy and digestive tract mega-syndromes develop (Ribeiro et al. 2012; Cunha-Neto and Chevillard 2014; Pérez-Molina and Molina 2018).

Despite affecting approximately 6–7 million people, and causing 14 thousand deaths per year in Central and South America, CD lacks effective vaccines; currently approved treatments are still limited to two obsolete nitroheterocyclic drugs, nifurtimox and benznidazole (BZN) (Moncayo and Silveira 2009; Hashimoto and Yoshioka 2012; Bern 2015). These drugs were developed more than 50 years ago and frequently fail to treat the disease (Sereno et al. 2004; Wilkinson et al. 2008; Mejia et al. 2012). Moreover, they elicit harmful toxic side effects and have extended treatment lengths (60–90 days) (Molina et al. 2014; Gaspar et al. 2015; Morillo et al. 2015; Morillo et al. 2017; Aldasoro et al. 2018). Therefore, the search for novel CD therapeutics is critical. The ideal target product profile (TPP) for CD includes (1) efficacy in both acute and chronic disease stages, (2) superior safety to BZN, (3) efficacy against all *T. cruzi* strains, (4) no drug interactions, and (5) affective oral treatment for 30 days (DNDi, 2019).

Nowadays, drug repositioning is a valuable approach for NTDs (Andrews et al. 2014). In this study, the trypanocidal activity of 21 repositioned leishmanicidal [1,2,3]Triazolo[1,5-a]pyridinium salts (Martín-Montes et al. 2017) was tested against three morphological forms of three different *T. cruzi* strains. The mode of action (MoA) of the trypanocidal compounds, **13**, **20** and **21**, was also evaluated, suggesting these compounds elicited *T. cruzi* cell death in a mitochondrion-dependent manner, through a bioenergetic collapse mechanism. In addition, **13** and **20** displayed significant selective inhibitors of iron-containing superoxide dismutase (Fe-SOD) of *T. cruzi*, a key enzyme in the elimination of reactive oxygen species and the protection from the damage produced by oxidative stress.

Materials and methods

Chemistry

The studied compounds **2–8** and **10–21** (Scheme 1) were described in our previous work (Martín-Montes et al. 2017). These compounds were synthesized from [1,2,3]triazolo[1,5-*a*]pyridine **1** and 3-methyl-[1,2,3]triazolo[1,5-*a*]pyridine **9** (Bower and Gramage 1957), prepared from commercial products, by reaction with the corresponding bromo compound.

In vitro trypanocidal activity assays

T. cruzi strains and culture

Epimastigote forms of three different *T. cruzi* strains—MHOM/Pe/2011/Arequipa (discrete typing unit (DTU) V) (Martín-Escolano et al. 2018), IRHOD/CO/2008/SN3 (DTU I) (Téllez-Meneses et al. 2008) and TINF/CH/1956/Tulahuen (DTU VI) (Martín-Escolano et al. 2018)—were cultured at 28 °C in Gibco® RPMI 1640 Medium supplemented with 10% (v/v) heat-inactivated foetal bovine serum (FBS), 0.03 M haemin and 0.5% (*w*/*v*) BBL trypticase (Kendall et al. 1990).

Trypanocidal activity against extracellular epimastigote forms

BZN and compounds to be tested were dissolved in 0.1% (v/v) DMSO (Panreac, Barcelona, Spain) and then assayed as nontoxic DMSO concentrations on cell growth. Trypanocidal activity was tested in 96-well microtiter plates as previously described (Martín-Escolano et al. 2018). Briefly, parasites collected in the exponential growth phase were seeded at 5×10^5 mL^{-1} after adding the tested compounds at dosages ranged from 400 to 1 μM in 200 mL $well^{-1}$ at 28 °C for 48 h. BZN and untreated growth controls were also included. Thereafter, resazurin sodium salt (Sigma-Aldrich) was added to be incubated for further 24 h. Finally, the trypanocidal effect was determined by absorbance measurements (Sunrise readerTM, TECAN), and the activity was expressed as the IC_{50} (concentration required to result in 50% inhibition) using GraphPad Prism 6 software. Each compound concentration was tested in triplicate in four separate determinations.

Cytotoxicity test on Vero cells

Mammalian Vero cells (EACC No. 84113001) were cultured at 37 °C in 95% humidified air and 5% CO_2 atmosphere in Gibco® RPMI 1640 Medium supplemented with 10% (v/v) heat-inactivated FBS (Pless-Petig et al. 2012). Cytotoxicity tests against Vero cells were performed in 96-well microtiter plates as described previously (Martín-Escolano et al. 2018).

Scheme 1 Synthesis of compounds **2–8** and **10–21**

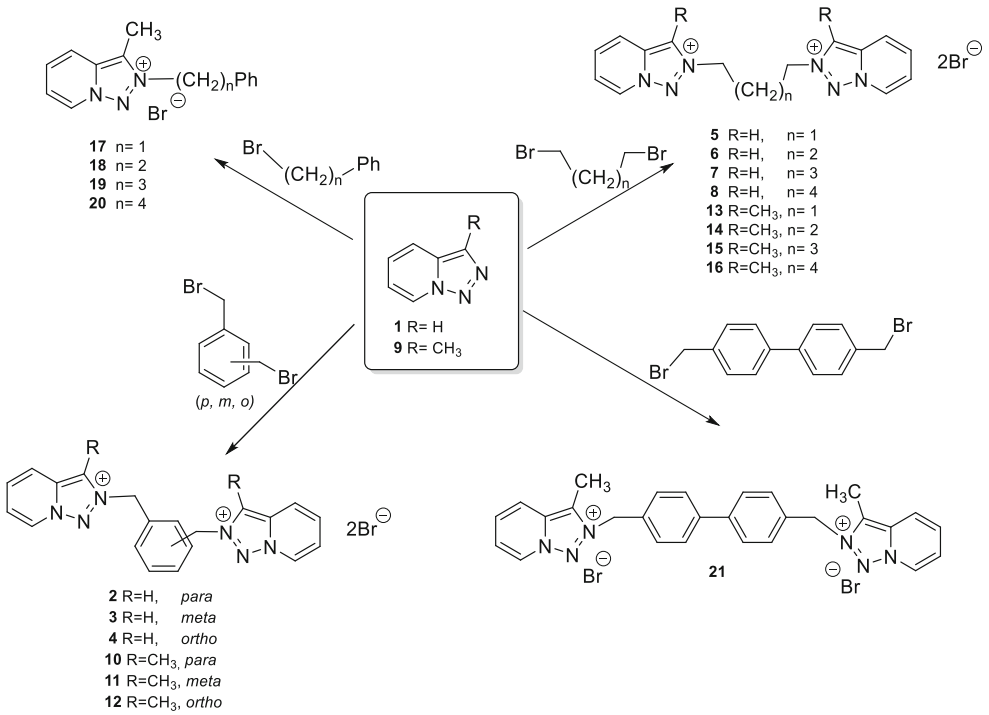

Briefly, Vero cells were seeded at 1.25×10^4 mL^{-1}, and after 24 h were treated by adding the tested compounds at dosages ranged from 3000 to 50 μM in 200 mL well^{-1} at 37 °C for 48 h. BZN and untreated growth controls were also included. Thereafter, resazurin sodium salt (Sigma-Aldrich) was added, and after 24 h of incubation, the same procedure as described to assess the trypanocidal activity in the epimastigote forms was carried out to determine the cell viability. Each compound concentration was tested in triplicate in four separate determinations.

Trypanocidal activity against intracellular amastigote forms

Trypanocidal activity was determined in 24-well microtiter plates using rounded coverslips according to the literature (Martín-Escolano et al. 2019c). Briefly, culture-derived trypomastigotes (obtained as previously described (Martín-Escolano et al. 2018)) were used to infect 1×10^4 Vero cells well^{-1} at a multiplicity of infection (MOI) ratio of 10:1 for 24 h. After that, the plates were washed of non-phagocyted trypomastigotes and treated by adding the tested compounds at dosages ranged from 50 to 1 μM in 500 mL well^{-1} at 37 °C in 95% humidified air and 5% CO_2 atmosphere for 72 h. BZN and untreated growth controls were also included. Finally, the trypanocidal effect was determined by counting the number of amastigotes in 500 host cells randomly distributed in microscopic fields in methanol-fixed and Giemsa-stained preparations. The activity was expressed as the IC_{50} using GraphPad Prism 6 software. Each compound concentration was tested in triplicate in four separate determinations.

Trypanocidal activity against bloodstream trypomastigote forms

Bloodstream trypomastigotes obtained by cardiac puncture from infected BALB/c mice during the parasitaemia peak in a 7:3 blood/anticoagulant (3.2% sodium citrate) ratio were used to perform this assay (Martín-Escolano et al. 2018). Trypanocidal activity was tested in 96-well microtiter plates according to the method previously described (Martín-Escolano et al. 2019c) by seeding the parasites at 2×10^6 trypomastigotes mL^{-1} and treating at dosages ranged from 50 to 1 μM in 200 mL·well^{-1} at 37 °C in 95% humidified air and 5% CO_2 atmosphere for 24 h. BZN and untreated growth controls were also included. Thereafter, resazurin sodium salt (Sigma-Aldrich) was added to be incubated for further 4 h. Finally, the same procedure as described to assess the trypanocidal activity in the epimastigote forms was carried out. Each compound concentration was tested in triplicate in four separate determinations.

MoA studies

^{1}H nuclear magnetic resonance (NMR) analysis of excreted metabolites

Epimastigotes of *T. cruzi* Arequipa strain were collected in the exponential growth phase and cultured at 5×10^5 ml^{-1} in 25 cm^2 cell culture flasks after adding the tested compounds at IC_{25} concentrations in 5 mL flask^{-1} at 28 °C for 72 h. Untreated controls were also included. Thereafter, centrifuged

and filtered supernatants were used for the ^{1}H NMR analysis of the excreted metabolites using a NMR spectrometer (VARIAN DIRECT DRIVE 500 MHz Bruker) as previously described (Fernández-Becerra et al. 1997). Chemical shifts were expressed in parts per million (ppm), and the binning and normalisations were achieved using Mestrenova 9.0 software, also using the human metabolome database (http://www.hmdb.ca/) for this purpose (Fernández-Becerra et al. 1997).

Flow cytometry analysis of mitochondrial membrane potential and nucleic acid levels

The untreated and treated epimastigotes of *T. cruzi* Arequipa strain described in the NMR analysis were collected, washed three times in PBS and stained with 10 mg mL^{-1} rhodamine 123 (Rho) (Sigma-Aldrich) or acridine orange (AO) (Sigma-Aldrich) dyes in 0.5 mL PBS at 28 °C for 20 min (Sandes et al. 2014). Non-stained parasites and potassium cyanide (KCN)–treated parasites (Abengózar et al. 2017) were also included. After elapsed time, epimastigotes were immediately washed twice in ice-cold PBS and dispersed in 1 mL of cold PBS for the fluorescence analysis using a flow cytometer (BECTON DICKINSON FACSAria III) and a FACSDiva v8.01 software (BECTON DICKINSON) (Martín-Escolano et al. 2018). Finally, the fluorescence intensities of Rho (FITC-A) and AO (APC-A) were quantified as described elsewhere (Sandes et al. 2014). The alterations in the fluorescence intensities were expressed as the index of variation (IV): IV = (TM–CM)/CM, where TM and CM are the median fluorescence for treated and untreated epimastigotes, respectively (Sandes et al. 2014).

Superoxide dismutase (SOD) enzymatic inhibition analysis

To obtain the Fe-SOD protein, epimastigotes of *T. cruzi* Arequipa strain collected in the exponential growth phase were cultured at 5×10^{9} ml^{-1} in 75 cm^{2} cell culture flasks in Gibco® RPMI 1640 Medium without FBS at 28 °C for 28 h. Thereafter, centrifuged and filtered supernatant was processed as described elsewhere (López-Céspedes et al. 2011). Finally, the protein content was quantified using the Bradford reagent (Sigma-Aldrich) (Bradford 1976) with bovine serum albumin (BSA) as a standard.

The in vitro activities of either excreted Fe-SOD and commercial Cu/Zn-SOD from human erythrocytes (Sigma-Aldrich) exposed to the tested compounds at a concentration range from 100 to 0.1 μM were determined using the method described elsewhere (Beyer and Fridovich 1987).

Molecular docking study

The compounds protonation state at pH 7.4 was estimated by the chemicalize web server (http://www.chemicalize.org/), and afterwards, they were designed with the program Avogadro (Hanwell et al. 2012). AM1 charges were calculated with the Chimera software (Pettersen et al. 2004). As targets for the docking, both the mitochondrial and cytosolic *T. cruzi* Fe-SOD protein structures were used (PDB entries 4DVH and 2GPC, respectively). For the first one, the residue numbering refers to that of Martinez et.al, i.e., without the mitochondrial signal peptide (Martinez et al. 2014). The protein protonation state at pH 7.4 was obtained with the program PDB2PQR (Dolinsky et al. 2007), and Gasteiger charges for the protein were added with Autodock (Morris et al. 2010). The docking study was performed with the Autodock4.0 program, using the Lamarckian genetic algorithm (LGA) (Huey et al. 2007), with a grid centred on the dimer interface, as defined in a previous article by our group (Moreno-Viguri et al. 2016).

Statistical analyses

SPSS software (v. 21, IBM) was used to perform the statistical analyses. The *t* test for paired samples was used to verify whether there were differences between the assays used: $p < 0.05$, 95% confidence level.

Results and discussion

In vitro trypanocidal activity

The wide genetic diversity of *T. cruzi* and its variable drug resistance to current treatments (Zingales et al. 2014; Zingales 2017) are important elements in the search for optimal trypanocidal compounds, as established the DND*i* (DNDi 2019). Therefore, three different strains—belonging to three different DTUs, from different locations, hosts and tropisms—with different genotypes and phenotypes (Martín-Escolano et al. 2018) were used to evaluate the trypanocidal activity of 21 [1,2,3]Triazolo[1,5-*a*]pyridinium salt compounds. In addition, these compounds were tested against the three morphological forms of this parasite. The replicative extracellular and easy-to-handle epimastigotes were used as a primary screening because of their ease of use and maintenance in the laboratory. Potentially useful compounds were identified and evaluated against amastigotes and trypomastigotes, these being the relevant *T. cruzi* forms responsible for acute and chronic stages of CD in mammalian hosts, respectively (Zingales 2017).

Trypanocidal activity, expressed as the IC_{50}, is shown (Table 1), together with data from the reference drug, BZN.

Table 1 Trypanocidal activity of benznidazole and compounds on the three developmental forms of *Trypanosoma cruzi* strains, and toxicity on mammalian Vero cells

Compound	Activity IC_{50} (μM)[a]			Activity IC_{50} (μM)[a]			Activity IC_{50} (μM)[a]			Toxicity IC_{50} (μM)[b] Vero cell
	T. cruzi Arequipa strain			*T. cruzi* SN3 strain			*T. cruzi* Tulahuen strain			
	Epim.	Am.	Trypom.	Epim.	Am.	Trypom.	Epim.	Ama.	Trypom.	
BZN	16.9 ± 1.8	8.3 ± 0.7	12.4 ± 1.1	36.2 ± 2.4	16.6 ± 1.4	36.1 ± 3.1	19.7 ± 1.7	10.0 ± 0.8	15.1 ± 1.3	80.4 ± 7.1
1	78.6 ± 5.9	nd	nd	105.2 ± 9.9	nd	nd	91.5 ± 7.2	nd	nd	845.8 ± 57.9
2	86.4 ± 11.1	nd	nd	124.3 ± 11.0	nd	nd	101.2 ± 12.9	nd	nd	1132.1 ± 84.0
3	46.5 ± 5.8	nd	nd	118.6 ± 14.5	nd	nd	51.6 ± 5.9	nd	nd	1309.7 ± 91.8
4	123.8 ± 14.0	nd	nd	253.6 ± 18.9	nd	nd	187.7 ± 21.8	nd	nd	727.0 ± 60.9
5	164.9 ± 18.7	nd	nd	245.0 ± 25.7	nd	nd	204.6 ± 25.1	nd	nd	987.5 ± 74.0
6	126.1 ± 16.6	nd	nd	235.8 ± 22.6	nd	nd	122.9 ± 15.9	nd	nd	1096.7 ± 91.2
7	116.9 ± 14.2	nd	nd	157.4 ± 14.5	nd	nd	184.3 ± 17.1	nd	nd	1112.7 ± 68.1
8	139.4 ± 16.9	nd	nd	166.3 ± 14.3	nd	nd	173.9 ± 19.4	nd	nd	2608.8 ± 134.3
9	61.4 ± 5.0	nd	nd	95.9 ± 8.6	nd	nd	121.8 ± 16.4	nd	nd	699.2 ± 40.9
10	35.4 ± 3.8	nd	nd	29.2 ± 1.7	31.2 ± 1.4	17.9 ± 1.6	21.2 ± 2.0	23.2 ± 1.0	16.8 ± 1.9	1396.6 ± 103.5
11	71.3 ± 8.1	nd	nd	260.1 ± 22.2	nd	nd	111.2 ± 14.3	nd	nd	1289.1 ± 104.7
12	42.0 ± 3.7	nd	nd	167.5 ± 19.0	nd	nd	62.8 ± 4.9	nd	nd	1214.3 ± 111.8
13	16.5 ± 2.2	19.6 ± 2.0	21.8 ± 1.9	7.7 ± 0.8	14.5 ± 2.7	13.9 ± 0.9	13.8 ± 1.0	18.1 ± 2.4	14.8 ± 1.1	1070.2 ± 94.3
14	206.9 ± 21.4	nd	nd	141.9 ± 12.8	nd	nd	378.2 ± 29.4	nd	nd	387.3 ± 21.9
15	170.5 ± 14.9	nd	nd	95.6 ± 10.1	nd	nd	154.6 ± 10.9	nd	nd	732.3 ± 57.9
16	91.8 ± 7.2	nd	nd	80.9 ± 6.5	nd	nd	140.2 ± 18.2	nd	nd	1808.2 ± 201.2
17	60.6 ± 4.9	nd	nd	50.0 ± 4.2	nd	nd	65.3 ± 4.5	nd	nd	1834.6 ± 141.3
18	122.4 ± 13.0	nd	nd	100.4 ±	nd	nd	132.1 ± 15.4	nd	nd	1513.4 ± 126.7
19	63.9 ± 7.8	nd	nd	88.6 ±	nd	nd	180.6 ± 19.8	nd	nd	1423.3 ± 109.4
20	14.2 ± 1.0	18.7 ± 1.8	15.9 ± 1.9	8.1 ± 1.1	12.3 ± 0.9	3.9 ± 0.5	11.4 ± 1.5	13.0 ± 1.7	8.2 ± 0.4	1537.5 ± 99.7
21	23.4 ± 3.1	24.3 ± 2.7	15.1 ± 1.3	8.8 ± 1.2	14.3 ± 1.5	6.2 ± 0.9	17.5 ± 2.7	19.5 ± 2.8	10.8 ± 0.7	1101.9 ± 91.2

Values are the means of three separate determinations ± standard deviation

BZN benznidazole, *nd* not determined

[a] Inhibition concentration 50 (IC_{50}), concentration (μM) required to inhibit 50% population, determined using GraphPad Prism 6

[b] Towards Vero cells

Cytotoxicity in mammalian VERO cells was also included to determine selectivity indices (SIs) of the compounds against *T. cruzi* (SI = IC_{50} Vero cells/IC_{50} parasite) (Table 2).

According to the literature, potential anti-Chagas agents must meet certain cut-off criteria: (1) $IC_{50} \leq 10$ μM and SI > 10 (Don and Ioset 2014), (2) SI > 50 (Nwaka et al. 2011), and (3) an efficacy non-inferior to BZN (DNDi 2019). Out of the 21 compounds screened this way, compounds **13**, **20** and **21** were selected for screening in amastigote and trypomastigote forms since they each exhibited IC_{50} values ranging from 7.7 to 23.4 μM, an SI > 50 and a higher trypanocidal efficacy than BZN. All tested compounds exhibited no cytotoxicity against VERO cells, with an $IC_{50} > 1000.0$ μM for most—approximately 12 times less toxic than BZN (IC_{50} = 80.4 μM).

The compounds selected for this study have the nucleus [1,2,3]triazolo[1,5-a]pyridine. Structurally, this heterocycle is completely different from that found in BZN; it also does not have any nitro groups implying less toxicity. The triazolopyridine salts were selected based on their synthetic accessibility and their solubility in water. To date, there are no studies on the toxicity of these systems in vivo, except those published by our group (Martín-Montes et al. 2017). In addition, BZN has been proved to be teratogenic (Castro et al. 2006), which stress on the development of alternative drugs. The compounds of this study (trizolopyridinium salts) are non-structurally related to BZN.

These three potential compounds were then tested against amastigote and trypomastigote *T. cruzi* forms—the relevant forms from a clinical point of view. These compounds continued to show trypanocidal activities better than BZN for at least half the clinical forms in the three strains. The effects on the BZN-resistant SN3 strain should be noted since the three compounds exhibited IC_{50} values < 15 μM and SI > 74 against all

Table 2 Selectivity index for benznidazole and compounds on the three developmental forms of *Trypanosoma cruzi* strains

Comp.	Selectivity index[a] *T. cruzi* Arequipa strain			Selectivity index[a] *T. cruzi* SN3 strain			Selectivity index[a] *T. cruzi* Tulahuen strain		
	Epim.	Am.	Trypom.	Epim.	Am.	Trypom.	Epim.	Am.	Trypom.
BZN	5	10	7	2	5	2	4	8	5
1	11 (2)	nd	Nd	8 (4)	nd	nd	9 (2)	nd	nd
2	13 (3)	nd	Nd	9 (4)	nd	nd	11 (3)	nd	nd
3	28 (6)	nd	Nd	11 (5)	nd	nd	25 (6)	nd	nd
4	6 (1)	nd	Nd	3 (2)	nd	nd	4 (1)	nd	nd
5	6 (1)	nd	Nd	4 (2)	nd	nd	5 (4)	nd	nd
6	9 (2)	nd	Nd	5 (2)	nd	nd	9 (1)	nd	nd
7	10 (2)	nd	Nd	7 (3)	nd	nd	6 (2)	nd	nd
8	19 (4)	nd	Nd	16 (8)	nd	nd	15 (8)	nd	nd
9	11 (2)	nd	Nd	7 (3)	nd	nd	6 (2)	nd	nd
10	39 (8)	nd	Nd	48 (24)	45 (9)	78 (39)	66 (17)	60 (8)	83 (17)
11	18 (4)	nd	Nd	5 (2)	nd	nd	12 (3)	nd	nd
12	29 (6)	nd	Nd	7 (3)	nd	nd	19 (5)	nd	nd
13	65 (13)	55 (6)	49 (7)	139 (70)	74 (15)	77 (39)	78 (20)	59 (7)	72 (14)
14	2 (0)	nd	Nd	3 (2)	nd	nd	1 (0)	nd	nd
15	4 (1)	nd	Nd	8 (4)	nd	nd	5 (1)	nd	nd
16	20 (4)	nd	Nd	22 (11)	nd	nd	13 (3)	nd	nd
17	30 (6)	nd	Nd	37 (19)	nd	nd	28 (7)	nd	nd
18	12 (3)	nd	Nd	15 (8)	nd	nd	11 (3)	nd	nd
19	22 (4)	nd	Nd	16 (8)	nd	nd	8 (2)	nd	nd
20	108 (22)	82 (8)	97 (14)	190 (95)	125 (25)	394 (197)	135 (34)	118 (15)	188 (38)
21	47 (9)	45 (5)	73 (10)	125 (63)	77 (15)	178 (89)	63 (16)	57 (7)	102 (20)

In brackets: number of times that compounds exceed the reference drug SI

nd not determined

[a] Selectivity index (SI), IC_{50} Vero cells/IC_{50} developmental forms of the parasite

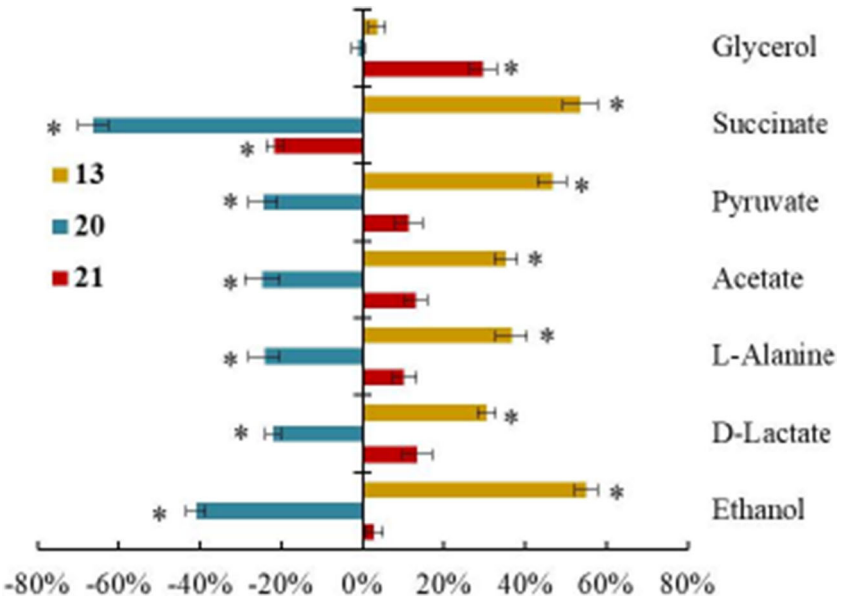

Fig. 1 Variation among peaks of catabolites excreted by epimastigote forms of *Trypanosoma cruzi* Arequipa strain exposed to **13**, **20** and **21** at IC_{25} concentrations in comparison to control (untreated) parasites incubated 72 h. Values constitute means of three separate determinations ± standard deviation. *Significant differences between untreated and treated parasites for $\alpha = 0.05$

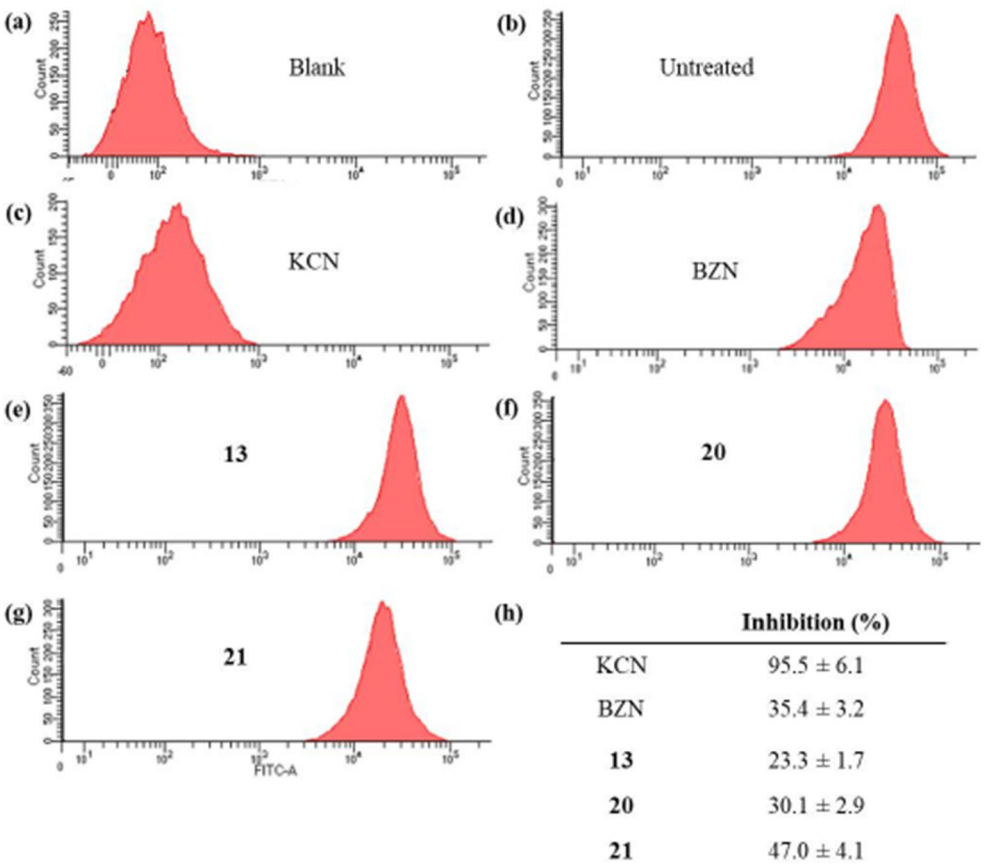

	Inhibition (%)
KCN	95.5 ± 6.1
BZN	35.4 ± 3.2
13	23.3 ± 1.7
20	30.1 ± 2.9
21	47.0 ± 4.1

Fig. 2 Mitochondrial membrane potential from epimastigote forms of *Trypanosoma cruzi* Arequipa strain exposed to benznidazole (BZN) and compounds at their IC_{25} concentrations incubated 72 h: **a** blank, **b** untreated (control), **c** potassium cyanide (KCN), **d** BZN, **e 13**, **f 20**, **g 21**. **h** Inhibition, in percentage, on mitochondrial membrane potential with respect to untreated parasites. Values constitute means of three separate determinations ± standard deviation. Significant differences between untreated and treated parasites for $\alpha = 0.05$

clinical forms. Therefore, a combinatorial therapy approach with BZN could avoid drug resistance and treatment failures. It is accepted that the cross-resistance of current treatments are based on BZN and nifurtimox, since both drugs must be activated by the same enzyme (i.e. mitochondrial type 1 nitroreductase) (Wilkinson et al. 2008; Mejia et al. 2012). A combined therapy using BZN and these compounds will be a multi-target therapy since these [1,2,3]Triazolo[1,5-*a*-]pyridinium salts present a MoA different from BZN (see below).

MoA studies

Catabolic alterations

MoA studies were performed at the glycolytic level, as trypanocidal activities exhibited by the [1,2,3]Triazolo[1,5-*a*-]pyridinium salts, **13**, **20** and **21**, could be derived from catabolic alterations, as described for leishmanicidal activity (Martín-Montes et al. 2017).

T. cruzi is unable to completely degrade glucose to CO_2 under aerobic conditions, excreting partially oxidised acids such as succinate or pyruvate, among others, into the medium (Bringaud et al. 2006; Maugeri et al. 2011). Therefore, different excreted metabolites were identified by ^{1}H NMR, and the spectra were measured and compared with metabolites from untreated parasites to evaluate the effects of the [1,2,3]Triazolo[1,5-*a*]pyridinium salts, **13**, **20** and **21** at IC_{25} concentrations (Fig. 1).

Glycerol, ethanol (end-products of alternative catabolic pathways) and succinate (one of the main glycolytic pathway end-products) were the most disturbed excretions for all tested compounds. These catabolic alterations are likely to be the result of a decreased mitochondrial ATP synthesis due to mitochondrial dysfunction, which is compensated for by an increased activity of the glycolytic pathway (the so-called Crabtree effect) (De Deken 1966). Alternative catabolic pathways could be activated to make up for energy deficits, thereby explaining alterations in glycerol and ethanol excretions (Bringaud et al. 2006). In addition, succinate excretion alterations could also be a consequence of redox stress, produced by Fe-SOD inhibition (Kirkinezos and Moraes 2001).

Mitochondrial dysfunction

To evaluate if catabolic alterations produced by the [1,2,3]Triazolo[1,5-*a*]pyridinium salts, **13**, **20** and **21**, were a consequence of mitochondrial dysfunction, parasites were treated at IC_{25} concentrations, as previously mentioned. Figure 2 shows flow cytometric analyses, including non-

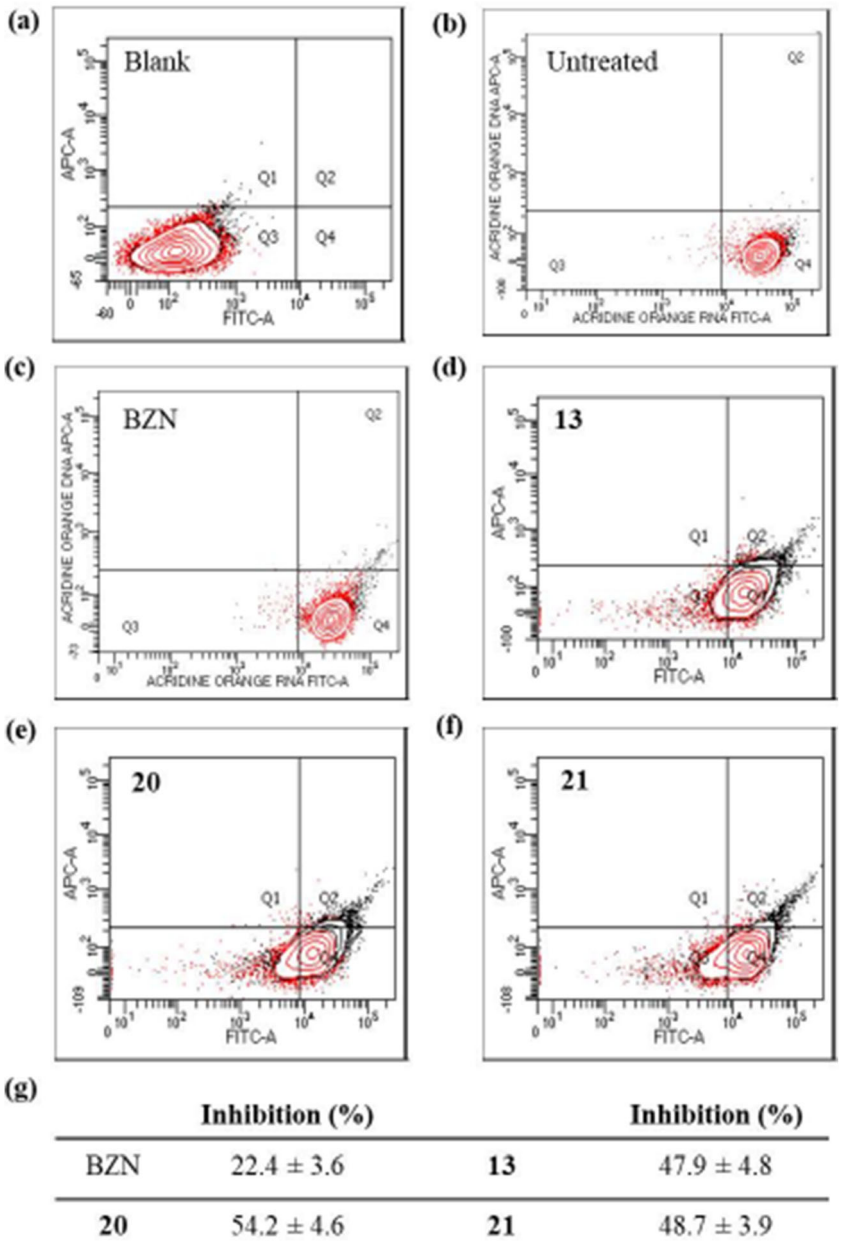

(g)

	Inhibition (%)		Inhibition (%)
BZN	22.4 ± 3.6	**13**	47.9 ± 4.8
20	54.2 ± 4.6	**21**	48.7 ± 3.9

Fig. 3 Nucleic acids levels of *Trypanosoma cruzi* Arequipa strain exposed to benznidazole (BZN) and compounds at their IC_{25} concentrations incubated 72 h: **a** blank, **b** untreated (control), **c** BZN, **d 13**, **e 20**, **f 21**. **g** Decrease, in percentage, in the nucleic acids levels with respect to untreated parasites. Values constitute means of three separate determinations ± standard deviation. Significant differences between untreated and treated parasites for $\alpha = 0.05$

stained parasites, non-treated parasites and parasites treated with BZN and KCN. KCN-treated parasites—a 10 mM KCN treatment for 40 min prior to Rho123 loading—were included as control samples with fully depolarised mitochondrion (Abengózar et al. 2017).

The data showed a membrane depolarisation of approximately 35.4% for BZN-treated parasites. Currently, it is accepted that BZN is metabolized by type I nitroreductases into glyoxal and other highly reactive metabolites (Hall and Wilkinson 2012), causing respiratory chain inhibition and the decrease in the mitochondrial membrane potential. Parasite treated with the tested compounds showed considerable depolarisation in the mitochondrial membrane, highlighting compound **21**, which caused higher depolarisation (47.0%) than BZN. As the mitochondrion plays mandatory roles in cell death (Lee and Thévenod 2006), and disturbances in mitochondrial membrane potential can cause imbalances in NADH/NAD^+ and ATP/ADP ratios, in addition to a reduction of nucleic acid levels (Michels et al. 2006; Verma et al. 2007), the cidal MoA of these compounds could be interpreted as a bioenergetics collapse before cell death, in a mitochondrion-dependent manner.

The decrease in ATP production due to the alteration of the membrane potential can affect DNA and RNA levels. Consequently, we determined nucleic acid levels in test parasites when compared with untreated controls, using flow cytometry for detecting fluorescence intensities of AO (Fig. 3). As expected, BZN-treated parasites showed a 22.4%

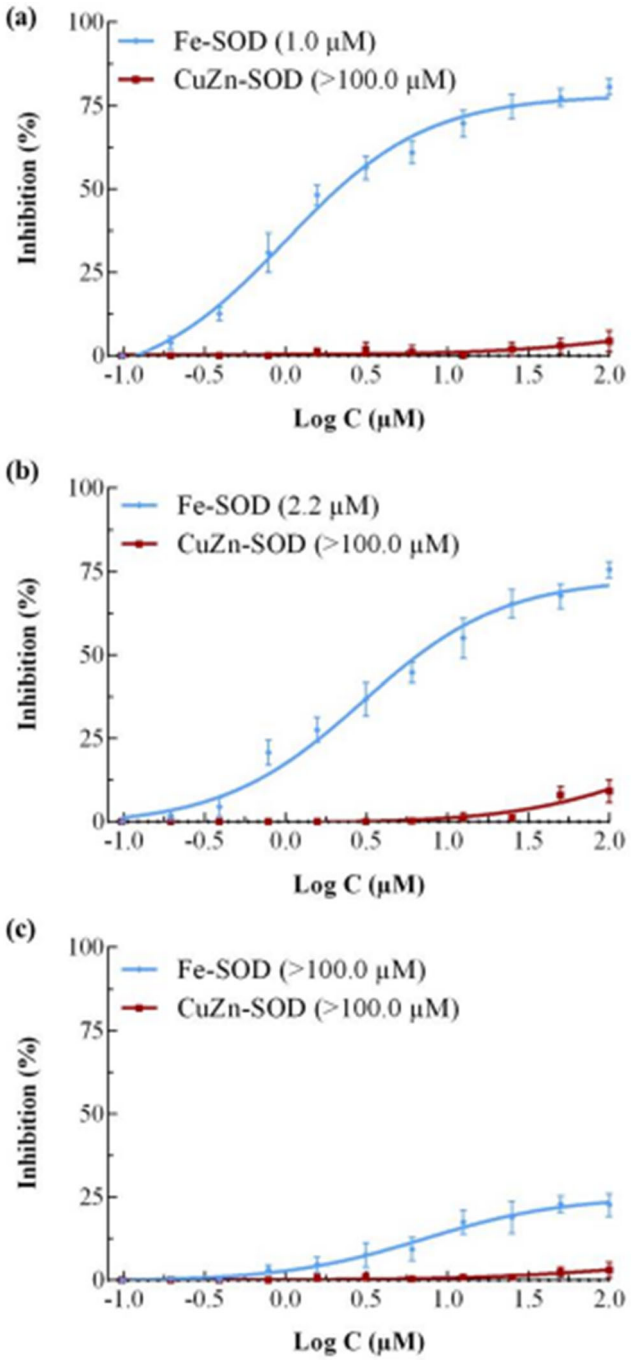

Fig. 4 In vitro inhibition (%) of *Trypanosoma cruzi* Fe-SOD (activity 42.0 ± 3.8 U mg^{-1}) and human erythrocytes CuZn-SOD (activity 47.3 ± 4.1 U·mg^{-1}) for **a 13**, **b 20** and **c 21**. Values constitute means of three separate determinations ± standard deviation. In brackets: IC_{50} value

reduction in nucleic acids levels (Martín-Escolano et al. 2019a, b), whereas parasites treated with compounds **13**, **20** and **21** showed greater reductions (approximately 50% for all three). Since the decrease in nucleic acids could be also due to random degradation due as a result of cell necrosis, the biological consequences of compounds were more than likely due to a cidal MoA.

SOD inhibition

Since the cidal MoA of compounds could be interpreted as a bioenergetic collapse in a mitochondrion-dependent manner, Fe-SOD inhibition assays were performed (Kirkinezos and Moraes 2001). Fe-SOD is a relevant therapeutic target for CD because of **a** its protective effects against reactive oxygen species (ROS) (Maes et al. 2004; Germonprez et al. 2005) and **b** its structural and biochemical differences with the human CuZn-SOD (Moreno-Viguri et al. 2016; Beltrán-Hortelano et al. 2017).

SOD inhibition curves produced by the three compounds are shown (Fig. 4). Considerable Fe-SOD inhibition was observed for compounds **13** and **20**, with no inhibitory effects on human CuZn-SOD. In contrast, compound **21** produced no inhibition on any SOD enzymes. Therefore, compounds **13** and **20** selectively inhibited Fe-SOD (IC_{50} values of 1.0 and 2.2 μM, respectively). Modelling studies were also performed to further investigate this process (Fig. 5). In contrast, the chance of multi-target compounds should not be rejected.

Compound molecular docking with *T. cruzi* Fe-SOD

While compounds **13**, **20** and **21** generated acceptable trypanocidal activities, only two inhibited Fe-SOD (**13** and **20**). To understand these different enzyme affinities, we performed docking experiments on all three compounds, using a previously published protocol by our group (Moreno-Viguri et al. 2016). Here, we present the results on the mitochondrial form, to help comparison with previous studies by us. Results on the cytosolic protein were very similar and are presented in Supplementary Figure S1. Our results showed similar binding modes for **13** and **20** (Fig. 5), similar to previous compounds (Moreno-Viguri et al. 2016; Martín-Escolano et al. 2018; Paucar et al. 2019). Those compounds bind deep in a cavity formed at the dimer interface, not far from the active site. While they do not interact with this site, nor with the iron metal, they could act by preventing substrate access to the active site (Moreno-Viguri et al. 2016; Muñoz et al. 2009) (Fig. 5d). The indol group binds to Phe123 of Fe-SOD and could potentially perform π-stacking interactions with this residue. The nitrogen group is involved in hydrogen bonds with both the side chain of Arg177 and the backbone of Asn122. The second indol group of compound **13**, similar to the phenyl of compound **20**, binds close to Pro178. This location was not observed in previous screens. However, we already showed that positioning of the second aromatic scaffold was variable, and that it could be substituted to an aliphatic group, without impacting on enzyme activity (Martín-Escolano et al. 2018; Paucar et al. 2019). The hydrophobic linker bound close to Trp165. Alternatively, compound **21** bound partially outside the cavity, far from Trp165 and Glu166, performing potential interactions barely with

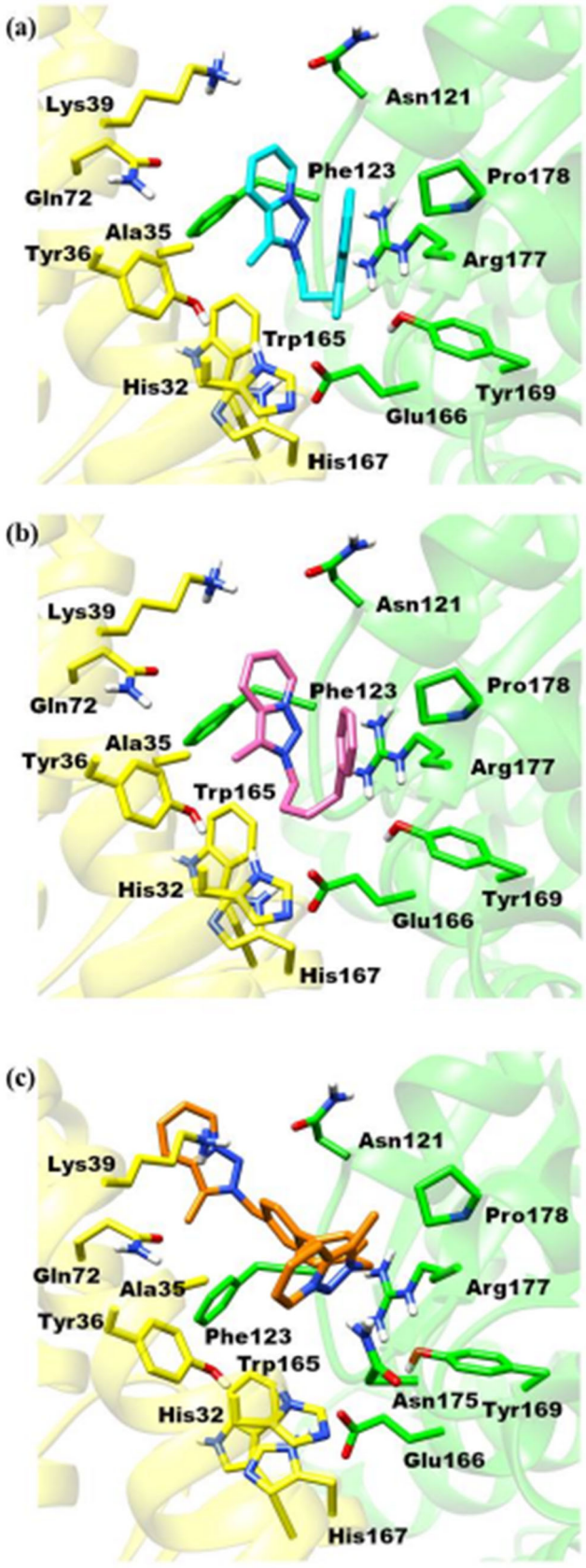

◀ **Fig. 5** Suggested binding mode for compounds **13** (**a**), **20** (**b**) and **21** (**c**), as obtained by molecular docking on the Fe-SOD enzyme (PDB ID 4DVH). The figures were created using the software package Chimera. In all the figures, one protomer is shown in yellow and the other in green. Iron ions are shown as brown spheres. Compounds are shown as sticks with carbon atoms in cyan (**13**), pink (**20**) and orange (**21**). **d** Hypothesis of the mode inhibition as suggested by docking, with compounds (represented here by compound **13**) binding in a cavity that seems to be the access of substrates to the active site. The two active site irons and their three coordinated histidines are shown. **e** In this image, all three compounds are shown bound in the cavity, close to the active site. The protein is shown as a surface, with the front plane removed to allow visualization of the cavity, whose internal surface is seen in grey. We can see how compounds **13** (cyan) and **20** (pink) bind deep, while compound **21** (orange) stays in the surface of the cavity. The images were created with The PyMol Molecular Graphics System, Schrödinger, LLC

Lys39 at one side, and with Pro178 and Asn175 at the other side (Fig. 5). The big rigid linker connecting the two indol groups did not allow for deeper binding inside the dimer interface, lying most surely as a reason for the observed lack of inhibition. Therefore, the activity of this compound (**21**) must be explained by another, still unknown target.

It should be noted that compounds **13**, **20** and **21** also were identified as potential leishmanicidal candidates for the treatment of leishmanisis. These compounds exhibited higher selectivity indexes than those of the reference drug Glucantime for the three *Leishmania* species evaluated: *L. braziliensis*, *L. infantum* and *L. donovani* (Martín-Montes et al. 2017). Moreover, these compounds showed to be selective inhibitors of the Fe-SOD in both parasites. Therefore, we can hypothesise that these [1,2,3]Triazolo[1,5-a]pyridinium salts are active against all trypanosomatids, and trials against *Trypanosoma brucei* should be conducted. Alternatively, assays using infected BALB/c mice will be performed in order to determinate the in vivo activity of these [1,2,3]Triazolo[1,5-a]pyridinium salts. If any of the compounds show in vivo activity, deeper investigations about the MoA will be performed.

In conclusion, we identified the [1,2,3]Triazolo[1,5-a]pyridinium salts, **13**, **20** and **21**, as cost-effective trypanocidal compounds for the development of new anti-Chagas therapeutic agents. In contrast to BZN, they had increased parasitic activities, an increased spectrum of action and lowered mammalian cytotoxicity. MoA analyses suggested that cidal activities were due to mitochondrion-dependent cell death via a bioenergetic collapse, caused by mitochondrial membrane depolarisation and Fe-SOD inhibition.

Authors' contributions RM-E and CM designed the study. RM-E, JM-E, RB-G and NC performed the experiments. RM-E, JM-E and NC collected and analysed the data. RM-E, RB-G and NC wrote the manuscript. RM-E, RB-G, BA, MJR, MS-M, RB and CM reviewed and edited the manuscript. All the authors discussed the results and contributed to the final manuscript.

Funding information This work was financially supported by the Ministerio de Economia, Industria y Competitividad (CONSOLIDER CSD2010–00065 and CTQ2017–90852-REDC), including funds from the European Regional Development Fundings (ERDF), Generalitat Valenciana Prometeo 2015/002 and from University of Valencia (Spain) (UV-INV-AE 15-332846). RM-E received an FPU Grant [FPU14/01537] from the Ministry of Education of Spain. Central Services for Experimental Research (SCSIE, Universitat de València) and U26 of ICTS NANBIOSIS platform provided the equipment employed.

Compliance with ethical standards

Conflict of interest The authors declare that they have no conflict of interest.

References

Abengózar MÁ, Cebrián R, Saugar JM et al (2017) Enterocin AS-48 AS evidence for the use of bacteriocins as new leishmanicidal agents. Antimicrob Agents Chemother 61:e02288–e02216

Aldasoro E, Posada E, Requena-Méndez A, Calvo-Cano A, Serret N, Casellas A, Sanz S, Soy D, Pinazo MJ, Gascon J (2018) What to expect and when: benznidazole toxicity in chronic Chagas' disease treatment. J Antimicrob Chemother 73:1060–1067

Andrews KT, Fisher G, Skinner-Adams TS (2014) Drug repurposing and human parasitic protozoan diseases. Int J Parasitol Drugs Drug Resist 4:95–111

Bastos CJC, Aras R, Mota G, et al (2010) Clinical outcomes of thirteen patients with acute Chagas disease acquired through oral transmission from two urban outbreaks in Northeastern Brazil 4:16–17

Beltrán-Hortelano I, Pérez-Silanes S, Galiano S (2017) Trypanothione reductase and superoxide dismutase as current drug targets for *Trypanosoma cruzi*: an overview of compounds with activity against Chagas disease. Curr Med Chem 24:1066–1138

Bern C (2015) Chagas' disease. N Engl J Med 373:456–466

Bern C, Montgomery SP (2009) An estimate of the burden of Chagas disease in the United States 30341:52–54

Bern C, Kjos S, Yabsley MJ, Montgomery SP (2011) *Trypanosoma cruzi* and chagas' disease in the United States. Clin Microbiol Rev 24:655–681

Beyer WF, Fridovich I (1987) Assaying for superoxide dismutase activity: some large consequences of minor changes in conditions. Anal Biochem 161:559–566

Blanchet D, Frédérique S, Schijman AG et al (2014) Infection, genetics and evolution first report of a family outbreak of Chagas disease in French Guiana and posttreatment follow-up. Infect Genet Evol 28:245–250

Bower JD, Gramage GR (1957) Heterocyclic systems related to pyrrocoline. Part II. The preparation of polyazaindenes by dehydrogenative cyclisations. J Chem Soc:4506–4510

Bradford MM (1976) A rapid and sensitive method for the quantitation of microgram quantities of protein utilizing the principle of protein-dye binding. Anal Biochem 72:248–254

Bringaud F, Rivière L, Coustou V (2006) Energy metabolism of trypanosomatids: adaptation to available carbon sources. Mol Biochem Parasitol 149:1–9

Cardillo F, Teixeira Pinho R, Zuquim Antas PR, Mengel J (2015) Immunity and immune modulation in *Trypanosoma cruzi* infection. Pathog Dis 73:ftv082

Castro JA, de Mecca MM, Bartel LC (2006) Toxic side effects of drugs used to treat Chagas' disease (American trypanosomiasis). Hum Exp Toxicol 25:471–479

Cunha-Neto E, Chevillard C (2014) Chagas disease cardiomyopathy: immunopathology and genetics. Mediat Inflamm 2014:683230

De Deken RH (1966) The Crabtree effect: a regulatory system in yeast. J Gen Microbiol 44:149–156

DNDi (2019) https://www.dndi.org/diseases-projects/chagas/%20chagas-target-product-profile/. Accessed 12/10/2019

Dolinsky TJ, Czodrowski P, Li H et al (2007) PDB2PQR: expanding and upgrading automated preparation of biomolecular structures for molecular simulations. Nucleic Acids Res 35:522–525

Don R, Ioset JR (2014) Screening strategies to identify new chemical diversity for drug development to treat kinetoplastid infections. Parasitology 141:140–146

Fernández-Becerra C, Sanchez-Moreno M, Osuna A, Opperdoes FR (1997) Comparative aspects of energy metabolism in plant Trypanosomatids. J Eukaryot Microbiol 44:523–529

Gaspar L, Moraes C, Freitas-Junior L, Ferrari S, Costantino L, Costi M, Coron R, Smith T, Siqueira-Neto J, McKerrow J, Cordeiro-da-Silva A (2015) Current and future chemotherapy for Chagas disease. Curr Med Chem 22:4293–4312

Germonprez N, Maes L, Van Puyvelde L et al (2005) *In vitro* and *in vivo* anti-leishmanial activity of triterpenoid saponins isolated from *Maesa balansae* and some chemical derivatives. J Med Chem 48:32–37

Hall BS, Wilkinson SR (2012) Activation of benznidazole by Trypanosomal type I nitroreductases results in glyoxal formation. Antimicrob Agents Chemother 56:115–123

Hanwell MD, Curtis DE, Lonie DC, Vandermeersch T, Zurek E, Hutchison GR (2012) Avogadro: an advanced semantic chemical editor, visualization, and analysis platform. J Cheminform 4:17

Hashimoto K, Yoshioka K (2012) Review: surveillance of Chagas disease. Adv Parasitol 79:375–428

Hernández C, Vera MJ, Cucunubá Z, Flórez C, Cantillo O, Buitrago LS, González MS, Ardila S, Dueñas LZ, Tovar R, Forero LF, Ramírez JD (2016) High-resolution molecular typing of two large outbreaks of acute Chagas disease in Colombia. J Infect Dis Adv 214:1252–1255

Huey R, Morris GM, Olson AJ, Goodsell DS (2007) Software news and update a semiempirical free energy force field with charge-based desolvation. J Comput Chem 28:1145–1152

Kendall G, Wilderspin AF, Ashall F, Miles MA, Kelly JM (1990) *Trypanosoma cruzi* glycosomal glyceraldehyde-3-phosphate dehydrogenase does not conform to the "hotspot" topogenic signal model. EMBO J 9:2751–2758

Kessler RL, Contreras VT, Marliére NP, Aparecida Guarneri A, Villamizar Silva LH, Mazzarotto GACA, Batista M, Soccol VT, Krieger MA, Probst CM (2017) Recently differentiated epimastigotes from *Trypanosoma cruzi* are infective to the mammalian host. Mol Microbiol 104:712–736

Kirkinezos IG, Moraes CT (2001) Reactive oxygen species and mitochondrial diseases. Semin Cell Dev Biol 12:449–457

L. B, J. M J, Y. C et al (2011) Chagas disease in european countries: the challenge of a surveillance system. Eurosurveillance 16:3

Lee W, Thévenod F (2006) A role for mitochondrial aquaporins in cellular life-and-death decisions? AJP Cell Physiol 291:C195–C202

López-Céspedes Á, Villagrán E, Briceño Álvarez K et al (2011) *Trypanosoma cruzi*: seroprevalence detection in suburban population of Santiago de Querétaro (Mexico). Sci World J 2012:914129

Maes L, Vanden Berghe D, Germonprez N et al (2004) *In vitro* and *in vivo* activities of a triterpenoid saponin extract (PX-6518) from the plant *Maesa balansae* against visceral *Leishmania* species. Antimicrob Agents Chemother 48:130–136

Martín-Escolano R, Moreno-Viguri E, Santivanez-Veliz M et al (2018) Second generation of Mannich base-type derivatives with *in vivo* activity against *Trypanosoma cruzi*. J Med Chem 61:5643–5663

Martín-Escolano R, Cebrián R, Martín-Escolano J, Rosales MJ, Maqueda M, Sánchez-Moreno M, Marín C (2019a) Insights into Chagas treatment based on the potential of bacteriocin AS-48. IJP Drugs Drug Resist 10:1–8

Martín-Escolano R, Marín C, Vega M, Martin-Montes Á, Medina-Carmona E, López C, Rotger C, Costa A, Sánchez-Moreno M

(2019b) Synthesis and biological evaluation of new long-chain squaramides as anti-chagasic agents in the BALB/c mouse model. Bioorganic Med Chem 27:865–879

Martín-Escolano R, Molina-Carreño D, Delgado-Pinar E, Martin-Montes Á, Clares MP, Medina-Carmona E, Pitarch-Jarque J, Martín-Escolano J, Rosales MJ, García-España E, Sánchez-Moreno M, Marín C (2019c) New polyamine drugs as more effective antichagas agents than benznidazole in both the acute and chronic phases. Eur J Med Chem 164:27–46

Martinez A, Peluffo G, Petruk AA, Hugo M, Piñeyro D, Demicheli V, Moreno DM, Lima A, Batthyány C, Durán R, Robello C, Martí MA, Larrieux N, Buschiazzo A, Trujillo M, Radi R, Piacenza L (2014) Structural and molecular basis of the peroxynitrite-mediated nitration and inactivation of *Trypanosoma cruzi* iron-superoxide dismutases (FE-SODs) A and B : disparate susceptibilities due to the repair of Tyr35 radical by Cys83 in FE-SODB through intramolecular electron transfer. J Biol Chem 289:12760–12778

Martín-Montes Á, Ballesteros-Garrido R, Martín-Escolano R, Marín C, Guitiérrez-Sánchez R, Abarca B, Ballesteros R, Sanchez-Moreno M (2017) Synthesis and *in vitro* leishmanicidal activity of novel [1,2,3]triazolo[1,5-a]pyridine salts. RSC Adv 7:15715–15726

Maugeri DA, Cannata JJB, Cazzulo JJ (2011) Glucose metabolism in *Trypanosoma cruzi*. Essays Biochem 51:15–30

Mejia AM, Hall BS, Taylor MC, Gómez-Palacio A, Wilkinson SR, Triana-Chávez O, Kelly JM (2012) Benznidazole-resistance in *Trypanosoma cruzi* is a readily acquired trait that can arise independently in a single population. J Infect Dis 206:220–228

Michels PAM, Bringaud F, Herman M, Hannaert V (2006) Metabolic functions of glycosomes in trypanosomatids. Biochim Biophys Acta - Mol Cell Res 1763:1463–1477

Molina I, Gómez i Prat J, Salvador F, Treviño B, Sulleiro E, Serre N, Pou D, Roure S, Cabezos J, Valerio L, Blanco-Grau A, Sánchez-Montalvá A, Vidal X, Pahissa A (2014) Randomized trial of posaconazole and benznidazole for chronic Chagas' disease. N Engl J Med 370:1899–1908

Moncayo Á, Silveira AC (2009) Current epidemiological trends of Chagas disease in Latin America and future challenges in epidemiology, surveillance, and health policy. Mem Inst Oswaldo Cruz 104:17–30

Moreno-Viguri E, Jiménez-Montes C, Martín-Escolano R, Santivañez-Veliz M, Martin-Montes A, Azqueta A, Jimenez-Lopez M, Zamora Ledesma S, Cirauqui N, López de Ceráin A, Marín C, Sánchez-Moreno M, Pérez-Silanes S (2016) *In vitro* and *in vivo* anti-*Trypanosoma cruzi* activity of new arylamine Mannich base-type derivatives. J Med Chem 59:10929–10945

Morillo CA, Marin-Neto JA, Avezum A, Sosa-Estani S, Rassi A Jr, Rosas F, Villena E, Quiroz R, Bonilla R, Britto C, Guhl F, Velazquez E, Bonilla L, Meeks B, Rao-Melacini P, Pogue J, Mattos A, Lazdins J, Rassi A, Connolly SJ, Yusuf S, BENEFIT Investigators (2015) Randomized trial of Benznidazole for chronic Chagas' cardiomyopathy. N Engl J Med 373:1295–1306

Morillo CA, Waskin H, Sosa-Estani S, del Carmen Bangher M, Cuneo C, Milesi R, Mallagray M, Apt W, Beloscar J, Gascon J, Molina I, Echeverria LE, Colombo H, Perez-Molina JA, Wyss F, Meeks B, Bonilla LR, Gao P, Wei B, McCarthy M, Yusuf S, STOP-CHAGAS Investigators (2017) Benznidazole and posaconazole in eliminating parasites in asymptomatic *T. cruzic*: the STOP-CHAGAS Trial. J Am Coll Cardiol 69:939–947

Morris GM, Huey R, Lindstrom W et al (2010) AutoDock4 and AutoDockTools4: automated docking with selective receptor flexibility. J Comput Chem 30:2785–2791

Muñoz IG, Moran JF, Becana M, Montoya G (2009) The crystal structure of an eukaryotic iron superoxide dismutase suggests intersubunit cooperation during catalysis. Protein Sci 14:387–394

Nwaka S, Besson D, Ramirez B, Maes L, Matheeussen A, Bickle Q, Mansour NR, Yousif F, Townson S, Gokool S, Cho-Ngwa F, Samje M, Misra-Bhattacharya S, Murthy PK, Fakorede F, Paris JM, Yeates C, Ridley R, van Voorhis WC, Geary T (2011) Integrated dataset of screening hits against multiple neglected disease pathogens. PLoS Negl Trop Dis 5:e1412

Paucar R, Martín-Escolano R, Moreno-Viguri E, Cirauqui N, Rodrigues CR, Marín C, Sánchez-Moreno M, Pérez-Silanes S, Ravera M, Gabano E (2019) A step towards development of promising trypanocidal agents: synthesis, characterization and *in vitro* biological evaluation of ferrocenyl Mannich base-type derivatives. Eur J Med Chem 163:569–582

Pérez-Molina JA, Molina I (2018) Chagas disease. Lancet 391:82–94

Pérez-Molina JA, Norman F, López-Vélez R (2012) Chagas disease in non-endemic countries: epidemiology, clinical presentation and treatment. Curr Infect Dis Rep 14:263–274

Pettersen EF, Goddard TD, Huang CC, Couch GS, Greenblatt DM, Meng EC, Ferrin TE (2004) UCSF chimera - a visualization system for exploratory research and analysis. J Comput Chem 25:1605–1612

Pless-Petig G, Metzenmacher M, Türk TR, Rauen U (2012) Aggravation of cold-induced injury in Vero-B4 cells by RPMI 1640 medium - identification of the responsible medium components. BMC Biotechnol 12:73

Requena-Méndez A, Aldasoro E, de Lazzari E, Sicuri E, Brown M, Moore DAJ, Gascon J, Muñoz J (2015) Prevalence of Chagas disease in Latin-American migrants living in Europe: a systematic review and meta-analysis. PLoS Negl Trop Dis 9:e0003540

Ribeiro AL, Maria P, Teixeira MM, Rocha MOC (2012) Diagnosis and management of Chagas disease and cardiomyopathy. Nat Rev Cardiol 9:576–589

Sandes JM, Fontes A, Regis-da-Silva CG, de Castro MCAB, Lima-Junior CG, Silva FPL, Vasconcellos MLAA, Figueiredo RCBQ (2014) *Trypanosoma cruzi* cell death induced by the Morita-Baylis-Hillman adduct 3-hydroxy-2-methylene-3-(4-Nitrophenylpropanenitrile). PLoS One 9:e93936

Sereno D, Tibayrenc M, Villarreal D, Barnabe C (2004) Lack of correlation between *in vitro* susceptibility to Benznidazole and phylogenetic diversity of *Trypanosoma cruzi* , the agent of Chagas disease. Exp Parasitol 108:24–31

Tarleton RL (2015) CD8+ T cells in *Trypanosoma cruzi* infection. Semin Immunopathol 37:233–238

Téllez-Meneses J, Mejía-Jaramillo AM, Triana-Chávez O (2008) Biological characterization of *Trypanosoma cruzi* stocks from domestic and sylvatic vectors in Sierra Nevada of Santa Marta, Colombia. Acta Trop 108:26–34

Tyler KM, Engman DM (2001) The life cycle of *Trypanosoma cruzi* revisited. Int J Parasitol 31:472–481

Verma NK, Singh G, Dey CS (2007) Miltefosine induces apoptosis in arsenite-resistant *Leishmania donovani* promastigotes through mitochondrial dysfunction. Exp Parasitol 116:1–13

WHO (2019) Chagas disease (American trypanosomiasis) fact sheet. https://www.who.int/en/news-room/fact-sheets/detail/chagas-disease-(american-trypanosomiasis. Accessed 12/10/2019

Wilkinson SR, Taylor MC, Horn D, Kelly JM, Cheeseman I (2008) A mechanism for cross-resistance to nifurtimox and benznidazole in trypanosomes. Proc Natl Acad Sci U S A 105:5022–5027

Zingales B (2017) Trypanosoma cruzi genetic diversity: something new for something known about Chagas disease manifestations, serodiagnosis and drug sensitivity. Acta Trop S0001-706X(17)30426–6

Zingales B, Miles MA, Moraes CB, Luquetti A, Guhl F, Schijman AG, Ribeiro I, Drugs for Neglected Disease Initiative, Chagas Clinical Research Platform Meeting (2014) Drug discovery for Chagas disease should consider *Trypanosoma cruzi* strain diversity. Mem Inst Oswaldo Cruz 109:828–883